2023 International Conference on Unmanned Aircraft Systems (ICUAS)
June 6-9, 2023 | Lazarski University, Warsaw, Poland

2023 International Conference on Unmanned Aircraft Systems (ICUAS) | 979-8-3503-1037-5/23/$31.00 ©2023 IEEE | DOI: 10.1109/ICUAS57906.2023.10156565

A Vision-based Approach for Unmanned Aerial Vehicles to Track Industrial Pipes for Inspection Tasks

Sara Roos-Hoefgeest[1], Jonathan Cacace[2], Vincenzo Scognamiglio[2], Ignacio Álvarez[1], Rafael C. González[1], Fabio Ruggiero[2] and Vincenzo Lippiello[2]

***Abstract*— Inspecting and maintaining industrial plants is an important and emerging field in robotics. A particular case is represented by the inspection of oil and gas refinery facilities consisting of different long pipe racks to be inspected repeatedly. This task is costly in terms of human safety and operation costs due to the high altitude location in which the pipes are placed. In this domain, we propose a visual inspection system for unmanned aerial vehicles (UAVs), allowing the autonomous tracking and navigation of the center line of the industrial pipe. The proposed approach exploits a depth sensor to generate the control data for the aerial platform and, at the same time, highlight possible pipe defects. A set of simulated and real experiments in a GPS-denied environment have been carried out to validate the visual inspection system.**

I. Introduction

The transport of fluids like steam, heating water and oil or liquid chemicals is made through a network of pipelines. Pipelines are typically grouped in a steel-framed structure called pipe racks (see Fig. 1). Typically, pipe racks are laid between different units in any chemical processing or power plant and are placed on elevated locations to preserve the ground space of the plant used for operators' mobility. Pipelines must be regularly inspected to assess their external/internal status. Their damage can be detected as a weakening of the external covering or the corrosion of its structure (i.e., rust on the pipe surface). Besides, damaged pipes can cause dangerous situations like explosions or chemical incidents. Pipeline cracks in oil and gas companies produce financial loss and environmental pollution rather than heavy casualties. For this reason, the early detection of defective pipe sections plays a crucial role in preventing unnecessary loss faced by oil and gas companies, ensuring safe working conditions as well. However, pipe racks often extend for miles and are located on elevated structures. Visually inspecting all the sections of the pipes is an expensive and demanding task. In particular, manual inspection of pipelines can be done regularly, but it is time-consuming and unsafe in hazardous areas. In addition, expensive scaffolding should be assembled to allow operators to reach inspection points.

Fig. 1: Pipe racks structures

In this context, using unmanned aerial vehicles (UAVs) equipped with vision sensors represents a low-cost and reliable solution to perform similar inspection tasks [1], [2]. Aerial systems can follow the surface of the pipelines, processing the information captured from a vision sensor to detect eventual defects. Automating such a task is not trivial, and different challenges must be addressed. First, the drone should be able to see the pipe to inspect and consequently follow its shape, regulating its position and orientation to track the pipeline. At the same time, during the navigation of the UAV, pipe defects must be detected. Different flaws can be present in the pipe structure, both externally and internally. In the latter case, the internal structure of the pipe is corrupted, and its thickness decreases. Here, the defects are detected using conventional non-destructive testing (NDT) with ultrasonic probes in contact with the inspected surface. Differently, our work focuses on external corrosion flaws visible on the pipeline structures.

This work's main contributions are the definition of a computer vision technique to detect and characterize pipeline structures, a UAV navigation strategy to track the pipes' surface and a method to highlight pipe defects based on vision data autonomously. A simulated case study using different pipe shapes has been carried out based on ROS and Gazebo [3], [4] simulator. Preliminary real-world experiments in a GPS-denied environment have also been performed to demonstrate approach effectiveness.

The remainder of the paper is organized as follows. In Section II, a brief overview of related works is presented while, in Section III, the sensor elaboration module to detect and extract salient information on the pipelines is discussed along with the UAV navigation controller strategy. Section IV describes the system architecture and, finally, Section V presents simulated and real-world experiments.

The research leading to these results has been supported by the AERIAL-CORE project, European Union's Horizon 2020 research and innovation programme under Grant Agreement No 871479; the AERO-TRAIN project, European Union's Horizon 2020 research and innovation programme under the Marie Skłodowska-Curie grant agreement No 953454; the scholarship under the "Severo Ochoa" program for predoctoral research and teaching with Ref: PA-20-PF-BP19-067, financed by Asturias Regional Government. The authors are solely responsible for its content.

[1]Department of Electrical, Computer Electronics and Systems Engineering, University of Oviedo, Asturias, Spain

[2]PRISMA Lab and CREATE Consortium, Department of Electrical Engineering and Information Technology, University of Naples Federico II, Naples, Italy.

II. Related Works

Pipelines damages can be caused by several natural and artificial factors, like overgrown vegetation, material deterioration or internal and external corrosion, among others [5]. Even though some of these causes are not predictable, inspecting pipelines can be essential in early damage detection and preventive maintenance. In this context, nowadays, pipelines are visually inspected or inspected by contact (i.e., using ultrasonic probes) with specialized operators walking close to the pipes on pre-built structures [6].

For this reason, in this work, we propose a comprehensive pipe inspection system that combines surface detection, tracking, and defect detection. In this context, different robotic and mechatronic solutions have been proposed to simplify the inspection task [7] that can also work in direct contact with the pipe surface. Robots that can directly walk internally [8]–[10] or externally [11]–[15] the pipeline have been developed. These robots can climb the surface to inspect adhering to it due to particular magnetic mechanisms to get information from the material integrity. For instance, in [16], the authors proposed an open-source car-like robotic platform to inspect internal pipe sections using an ultrasonic sensor. These solutions are not helpful when the pipes are placed in altitude locations due to the difficulties in reaching the inspecting surfaces. Moreover, magnetic wheels can not work if the tube presents external insulation. For this reason, the most prominent technology adopted to accomplish inspection tasks considers using UAVs. Aerial vehicles can hover in the air and are highly versatile systems that have been extensively used in different applications related to the inspection of industrial plants [17], [18].

Several works propose UAV applications to inspect industrial pipes close to our domain. In [19], the authors proposed a method to coordinate UAVs with maintenance crews to alert when a failure is detected. However, only the coordination phase between the ground crew and the UAVs is considered. In [20], pipeline structures are used to improve the localization performance of a UAV in the GPS-denied environment of industrial facilities. There, only numerical results were presented. A control approach to solving the pipeline tracking problem is presented in [21], while an application similar to the one presented in this paper is proposed in [22]. In this latter work, authors rely on deep learning techniques to segment the industrial pipes and gather video data to analyze offline to detect structural defects and the control of the UAV is not considered.

As for damage detection, many solutions have been deployed exploiting different sensors. The most diffuse is the camera sensors, like the one used in our application. In [23] and [24], the authors develop a neural network to detect corrosion in water, oil and gas pipelines. However, only data elaboration is considered without considering the pipe detection and tracking processes. Differently, we rely on model-based approaches to assess the status of the pipe. Other approaches consider the use of thermal camera sensors [25], [26] or NDT performed with UAVs [27], [28].

III. Modules Description

This paper presents a visual inspection system for UAVs that enables autonomous detection and navigation along the centre line of pipelines. The proposed approach exploits an RGB-D camera that provides image and depth data to generate control input for the aerial platform. Figure 2 shows the reference frames of the system.

First, the pipe to inspect is detected and characterized. To this scope, the location and the shape of the pipe must be identified. This information is crucial for determining the starting point of the inspection path and direction. This information provides the initial inspection point for the UAV. Then, the inspection is performed using a vision-based approach, in which the drone follows the shape of the pipe while capturing information from it using an inspection sensor. To follow the shape of the pipe, the UAV is commanded to maintain a path along the central axis of the pipe in the inspection direction. In this context, the axis of the pipe is extracted from the depth image, thanks to a combination of image processing techniques based on distance and pipe size parameters. The axis is then used to identify the next position and orientation to which the drone should navigate. This process is repeated for each camera frame to control the drone's motion throughout the entire inspection.

During the tracking process, the inspection sensor captures data for defect detection. Specifically, we present a preliminary, straightforward approach to detecting corrosion.

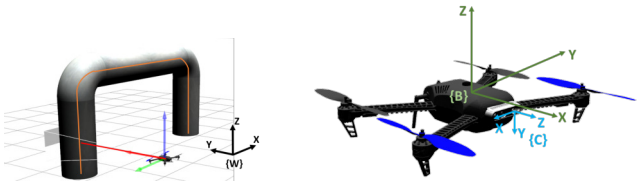

(a) (b)

Fig. 2: Drone, inspection sensor and world reference frames. Also, a pipe and first pose of the drone to start the inspection are shown.

A. Pipeline detection and characterization

The location of the pipe and its shape must be extracted from the depth sensor to start the inspection. One key aspect of the proposed approach is the ability to divide the pipe into different sections based on changes in shape and growth direction. Such an aspect enables specific inspections at different areas without the need for a full inspection of the pipeline. This way, defects in certain pipeline areas could be easily detected.

The first step is to cluster the different objects in the point cloud using a *region growing segmentation* algorithm. The point cloud is segmented into different clusters based on the similarity of the angles between the points' normal within each cluster. The algorithm starts with selecting an initial seed point and then iteratively adds nearby points with similar characteristics to the seed point to the cluster. This

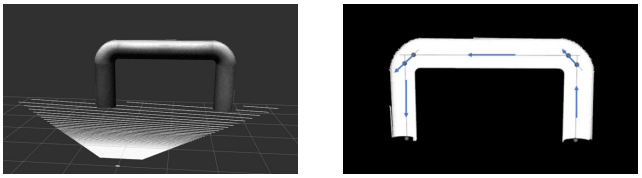

(a) (b)

Fig. 3: Pipeline detection and sectioning process. (a) Visualization of the point cloud of the scene. (b) Final result. Spheres indicate the starting and ending points of each section, and the arrows indicate their direction

algorithm helps identify the pipe in the point cloud data, as it can effectively separate it from other environmental surfaces. After this step, planar regions such as the floor and walls are filtered out to eliminate noise and improve the accuracy of pipeline localization.

In our system, the pipe structure is represented as a set of cylinders, each identifying a distinct section of the pipe with its own set of parameters. This method segments the pipe into various sections based on variations in shape and direction of growth. The process involves iteratively fitting cylinders to each group of points and refining the cylinder parameters until the entire pipe can be described as a combination of cylinders. We use an algorithm based on *random sample consensus* (RANSAC) [29] to fit the cylinders to the 3D points of the cluster. The obtained cylinders are defined with the following coefficients: a point in the cylinder axis, the axis direction vector, and the estimated radius.

After modelling each section of the pipe as cylinders, the boundaries of each section are determined by identifying the point at which the axes of consecutive sections intersect, based on their position in space, as illustrated in Fig. 3. The tracking algorithm uses this information to determine the drone's starting position and the direction of its scan.

B. Pipeline tracking

The vision-based pipe tracking method proposed in this work aims to monitor the central line of the pipe continuously. This method begins with the drone reaching the previously determined initial point of inspection, where the direction is also estimated in the previous step.

To this scope, the pipe is segmented with respect to the rest of the environment based on the depth information provided by the RGB-D sensor. During the inspection, the sensor is positioned close to the pipe. Therefore, the pipe is identified as the object closest to the camera. The closest points to the camera are selected from the depth information considering a range of distances, discarding objects far from the camera or small clusters due to sensor noise, including those between the sensor and the pipe. After this process, a binary image is obtained with the points belonging to this range (Figs.4a and 4b), including points close to the pipeline that are not necessarily part of it, see Fig. 4c. The image is processed by applying an opening morphological operation to remove small isolated pixels while preserving the overall shape of the pipe.

Finally, when more than one cluster is generated, the one with the most points is selected as the pipe. This is done using connected component analysis, which labels each connected component in the binary image and counts the number of pixels in each component.

The result of this process is a binary image, known as the mask image, in which the pixels associated with the pipe are assigned a value of 1 and all other pixels are assigned a value of 0 (see Fig. 4d).

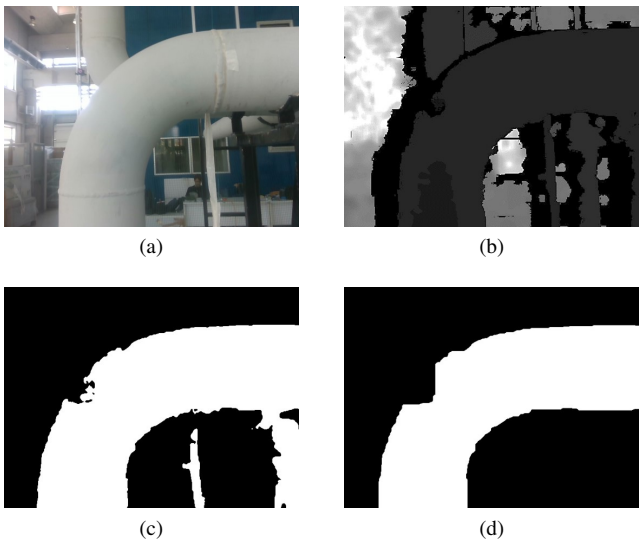

(a) (b) (c) (d)

Fig. 4: Process of obtaining the mask image of the pipe. (a) RGB image. (b) Depth image. (c) Resulting image after obtaining the nearest cluster to the camera. (d) Final result. Pixels in white belong to the pipe.

Once the pipe is identified, the method extracts its central axis. A thinning algorithm is applied to the binary mask to obtain the skeleton (see Fig.5a). The thinning algorithm is a morphological operation used to extract the centerline or skeleton of an object in a binary image. It works by iteratively removing pixels from the object's boundaries while preserving the overall structure of the object. This is achieved by using morphological operations such as erosion and dilation to selectively remove pixels until a thinned version of the object is obtained. However, the skeleton image obtained by the thinning algorithm may contain noise and inaccuracies, as can be seen in Fig. 5a. The distance transforms of the binary image are being considered to enhance the precision of the skeleton. The distance transform computes the shortest distance from each pixel to the closest non-zero pixel, as shown in Fig. 5b. This data is then employed to refine the accuracy of the skeleton by eliminating pixels with low distance transform values from the skeleton (see Fig. 5c).

After obtaining the skeleton of the pipe, the next step is to improve the skeleton and obtain a more accurate representation of the pipe's axis. Our approach uses a 3-degree polynomial fitting to approximate the skeleton points

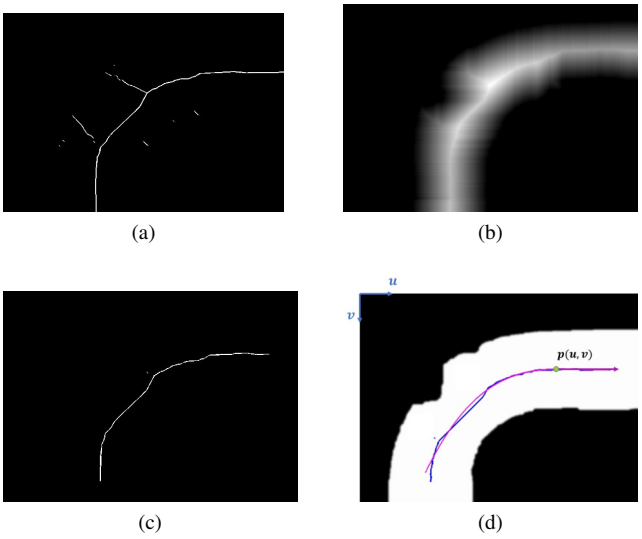

Fig. 5: Central axis extraction from pipe mask image and (a) Result of thinning algorithm. (b) Result of distance transform algorithm. (c) Pipe skeleton (d) Final result: Both skeleton (blue line) and final axis (pink line) in mask image. Also, green dot represents the tracking point.

according to equation 1.

$$y = a_0 + a_1 x + a_2 x^2 + a_3 x^3, \tag{1}$$

describing the polynomial fitting method used. The input is the skeleton of the pipe, which is represented as a set of points. The output is a smooth curve that provides a more accurate representation of the pipe's axis. a_0, a_1, a_2 and a_3 are the coefficients obtained by solving a linear least square problem, which minimizes the sum of the squares of the residuals between the data points and the polynomial function. Once the polynomial coefficients are obtained, the pipe axis pixels can be obtained by evaluating the polynomial function for the range of skeleton values. The degree of the polynomial affects the smoothness and precision of the curve. A 3-degree polynomial was selected to find the right compromise between the characteristics above for this application. The choice of the independent variable (x or y) in the polynomial function depends on the orientation of the pipe in the image. This can be determined by comparing the range of x and y coordinates.

The position and orientation of the drone to continue with the tracking in the next instant are estimated starting from this axis. For the position, one point is selected as the next tracking point. Accurately predicting the next tracking point during pipeline inspection is vital. Both the direction of the inspection and the pipeline are considered to guide the drone. The tracking point is selected in the direction of inspection and in line with the pipe growth. This point on the axis is transformed into a 3D point in the world reference frame to guide the drone. This process is repeated for each frame until the pipe inspection is complete. A pin-hole model is assumed to model the camera. According to this model, the vector $\mathbf{p}_p^{\mathcal{C}} \in \mathbb{R}^3$ describing the position of the point lying on the pipe in camera frame $\mathcal{C}$, recovered by using the 2D pixel $\mathbf{p}(u, v)$ the depth value $d(u, v)$ obtained from the depth map, and the intrinsic parameters of the camera using

$$\begin{aligned} p_{p,x}^{\mathcal{C}} &= d(u,v)((u - c_x) f_x^{-1}), \\ p_{p,y}^{\mathcal{C}} &= d(u,v)((v - c_y) f_y^{-1}), \\ p_{p,z}^{\mathcal{C}} &= d_{insp} - d(u,v), \end{aligned} \tag{2}$$

where (c_x, c_y) are the principal point of the camera and (f_x, f_y) the focal length of the camera in the x and y direction, respectively. Also, a minimum distance inspection (d_{insp}) is set considering drone construction factors, such as blade size, when determining the proximity distance to the pipeline.

The process of transforming a 3D point in the camera coordinate system to the world coordinate system involves utilizing the following

$$\mathbf{p}_d^{\mathcal{W}} = \mathbf{T}_{\mathcal{B}}^{\mathcal{W}} \mathbf{T}_{\mathcal{C}}^{\mathcal{B}} \mathbf{p}_p^{\mathcal{C}}. \tag{3}$$

This equation utilizes the extrinsic parameters of the camera, which include the rotation and translation of the camera with respect to the body frame of the drone $\mathcal{B}$, represented by the transformation matrix $\mathbf{T}_{\mathcal{C}}^{\mathcal{B}}$, obtained during the mounting of the camera on the drone. Additionally, the equation also utilizes the transformation matrix $\mathbf{T}_{\mathcal{B}}^{\mathcal{W}}$ between the body frame and the world frame $\mathcal{W}$, which is provided by the localization system. Combining these two transformation matrices allows the desired point to be transformed into the world coordinate system. Once the transformation is complete, the resulting point in the world coordinate system, represented by $\mathbf{p}_d^{\mathcal{W}}$, is sent to the drone controller.

The desired yaw angle ψ_d, which allows the drone to face the pipeline, is calculated based on the pipeline axis. The angle between the camera's z-axis and the pipeline direction axis should be 90 degrees. The following equation

$$\Delta_\psi = \text{acos}\left(\frac{\mathbf{v}_{axis} \times \mathbf{v}_{forward}}{\|\mathbf{v}_{axis}\| \ \|\mathbf{v}_{forward}\|}\right) \tag{4}$$

calculates the angle between the pipeline axis and the camera's forward direction. The pipeline axis is represented by the vector $\mathbf{v}_{axis}$, in the camera's reference frame, and it is obtained by subtracting the starting point of the axis from its ending point in the 3D space. The forward direction of the camera is represented by $\mathbf{v}_{forward}$, which is considered to be unitary in the z direction, i.e. $[0, 0, 1]$. By adjusting the current yaw angle of the drone with the calculated angle, the drone can be oriented towards the inspected pipe. This adjustment yields the desired yaw in the world reference coordinate system.

C. Defect detection

Defect detection is performed using the data recorded during the inspection. We present a straightforward approach to detecting corrosion by processing the RGB image captured during the inspection. In this work, our contribution mainly considers the capacity of the UAV to highlight possible corrupted areas of the pipe.

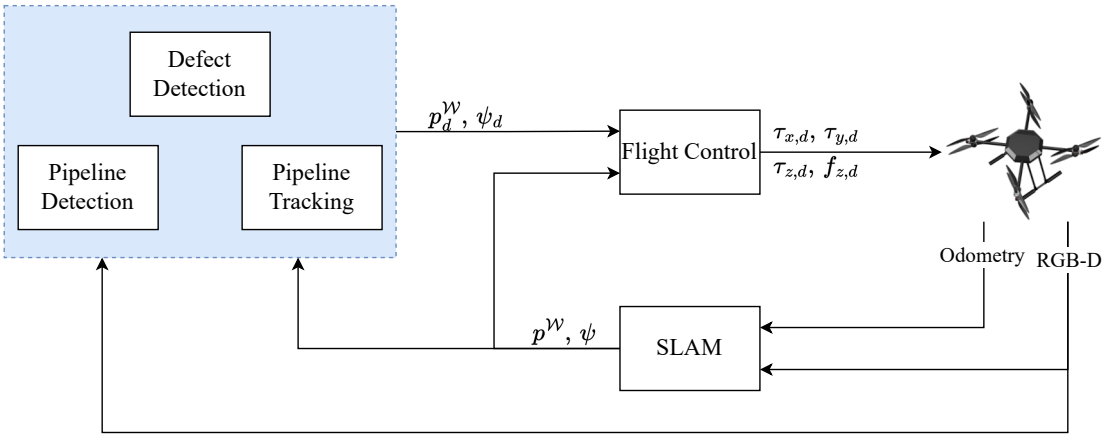

Fig. 6: System architecture

The first step of the detection algorithm aims to remove the colour of the pipeline from the image to identify potential defects in the pipeline. The pipeline colour is assumed to be the most frequent in the image and is used as a reference to differentiate it from the potential defects.

The pipe mask obtained during the tracking is applied to the RGB images only to retain the pixels corresponding to the pipe. Then, a medium blur is applied to the pipe image to reduce noise and smooth the image, which makes it easier to identify the colour of the pipe. The HSV colour space is considered to continue the image elaboration process. In this context, the hue channel represents the pixel's colour, while the saturation and value channels represent the intensity and brightness of the colour, respectively. By converting the image to the HSV colour space, we can separate the colour information from the saturation and brightness information, which makes it easier to identify the colour of the pipe.

The k-means clustering algorithm is used to group the pixels of the image into k clusters according to their colour and find the predominant colour of the pipeline. The number of clusters has been experimentally set to 4. The k-means algorithm is a widely used technique for clustering, which assigns each pixel to the cluster whose centroid (mean value) is closest to it.

We assume that the most significant cluster corresponds to the colour of the pipe, as it is the most frequent in the image that is then removed to leave only the potential defects. The output of the defect detection process is a new image in which the potential defects of the pipe are superimposed, as discussed in the case study section.

Once potential defects are identified, the next step is to search for corrosion by characterizing its color in the HSV color space and searching for corresponding color values within the image of potential defects. A common range of color values associated with corrosion is employed to achieve this task.

IV. System Architecture

The system architecture is depicted in Fig. 6. The main contribution of this work is grouped in the container with the azure background. As for the autonomy of the aerial system, the onboard Position Control module implemented on the UAV autopilot is used. The UAV is equipped with a standard PixHawk autopilot, running the PX4 control stack. The input of this module is the current position ($\mathbf{p}^{\mathcal{W}}$) with respect to a fixed frame, the heading orientation (namely, the yaw, ψ) and the desired ones ($\mathbf{p}_d^{\mathcal{W}}$, ψ_d), respectively. Running on onboard autopilot, this information is used to generate the attitude control signals used in the low-level control of the platform. As for the estimated current position, inspection and maintenance applications require precise vehicle localisation during the operation. In almost all industrial scenarios using a mobile robot, the global positioning system (GPS) is absent or very degraded, which means that alternative localisation methods are required to allow a drone to navigate in this kind of environment. Stricter are the requirements on the accuracy of the movements, and more critical becomes the role of the position estimation algorithm. For this reason, alternative state estimation systems are one of the most explored topics in the mobile robots field. When localisation via GPS is not reliable because the UAV operates in GPS-denied and GPS-spoofed environments, like the domain considered in this work due to the vicinity of iron structures, visual odometry or SLAM techniques can be adopted.

The SLAM module of the system architecture fuses platform motion odometry data with the depth sensor information to generate the estimated position $\mathbf{p}^{\mathcal{W}}$ and orientation ψ in the world frame. This information is exploited from the detection and tracking modules to generate the desired point to control the platform during the inspection task. In this context, the UAV is equipped with an Intel T265 tracking camera device [1] that directly provides an initial estimation of the 6 DOF pose of the platform (i.e. the odometry). Odometry is fused with the depth information from the Realsense D435 [2] depth sensor from the SLAM module. In this work, RTABMap [30] module is used.

[1] https://www.intelrealsense.com/tracking-camera-t265/

[2] https://www.intelrealsense.com/depth-camera-d435/

Finally, the estimated position, along with the sensor data from the depth sensor mounted on the UAV frame, are used firstly by the Pipeline Detection module to extract information from the pipe structure and later by the Pipeline Tracking module, which calculates the next point to navigate to follow the pipeline surface. Finally, image data from the depth sensor are used from the Defect Detection module of the system architecture to check the quality of the pipeline.

V. Case Studies

In order to evaluate the performance of the proposed framework for pipeline inspection, several experiments were conducted. The experiments were divided into two parts, simulation and real-world experiments.Video available online [3].

A. Simulations

The simulations were performed to experiment with different pipeline shapes and test the proposed approach in a controlled environment. The Gazebo simulator was used to replicate an environment with pipelines of various shapes, as well as to simulate the drone and inspection system. The aerial platform used in the simulation experiments is an Iris quadcopter, and the inspection sensor is a RealSense D435. The simulation environment and the simulated drone model can be seen in Fig. 7.

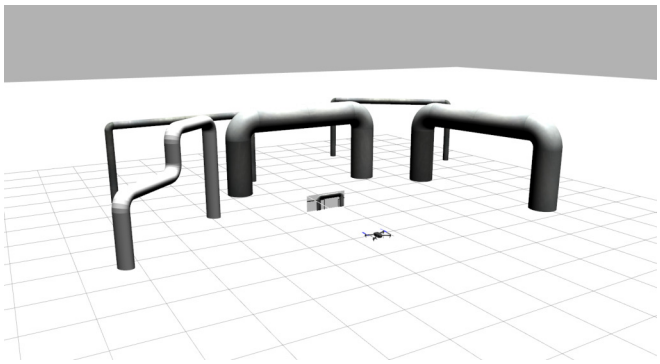

Fig. 7: Gazebo simulation environment with multiple pipes of different shapes.

Figure 8a shows the result of the pipe detection, where an orange circle marks the point selected as the starting point of inspection and an arrow points the direction in which the drone is supposed to move for further tracking. Fig.8b shows the path performed by the drone to reach the initial point of the inspection.

The results of pipeline tracking with multiple pipelines in the environment are presented in Fig.9. Instead, Figure 9a shows the simulated environment in Gazebo with several pipes one after the other. Figure 9b shows a frame captured during the tracking process of the pipe closest to the camera. The pink line represents the pipe's central axis, which has been extracted accurately by our algorithm. It can be observed that even in the presence of multiple pipes in the environment, the algorithm developed can correctly identify and track the pipe closest to the camera. The green dot represents the next tracking point selected from the centre axis; in this case, the drone moves downwards.

[3]https://www.youtube.com/watch?v=f16qlqEjVc0

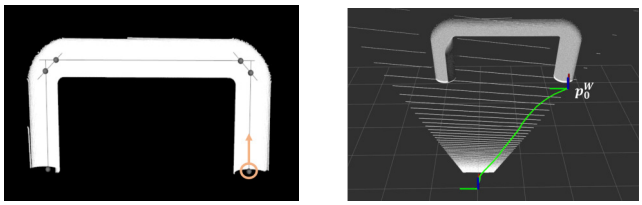

(a) (b)

Fig. 8: (a) Result of pipe detection. The orange circle marks the point chosen as the initial point of inspection, and the arrow marks the tracking direction. (b) Trajectory visualization. The trajectory followed by the drone to achieve the initial point of the inspection is shown in green.

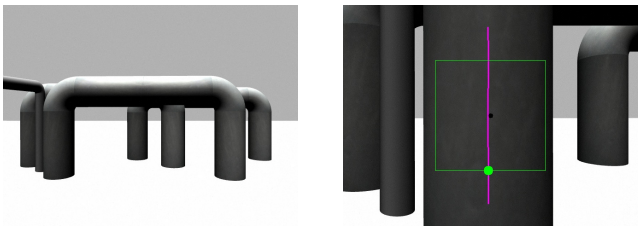

(a) (b)

Fig. 9: Experiment with different pipes in the same scene. The one in front is inspected. (a) Simulated scene in Gazebo. (b) A frame during the tracking process. The pink line represents the central axis of the pipe, and the green dot is the next tracking point.

As shown in Fig. 10, additional simulations were conducted to evaluate the performance of our algorithm on pipes of different shapes. The first one, shown in Fig. 10a, involves a pipe with a simple shape, while the second one, presented in Fig. 10b, features a pipe with a more complex shape.

The results of both simulations demonstrate the drone's capability to effectively follow the central axis of the pipes, enabling it to perform a comprehensive inspection. The complete trajectory of the drone is illustrated in green in both figures. These results further confirm the effectiveness of our algorithm in tracking objects of varying shapes and its potential for use in various industrial settings where accurate pipe inspection is essential.

B. Real-case experiments

The real-world experiments were conducted to test the proposed approach in a real-world scenario (see Fig. 11a). A quadcopter with an RGB-D camera and a tracking camera located at the front of the drone was used. As written before, the sensors chosen are the Realsense D435 for the depth information and a Realsense T265 for the tracking module. The tracking camera gave the odometry feedback input to RTABMap, which, using the information from the depth sensors, computed the position of the base link of the drone

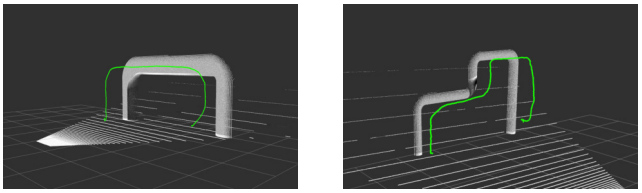

(a) (b)

Fig. 10: The trajectory performed by the UAV to inspect the pipe is shown in green in different experiments.

with respect to a fixed map frame. Figure 11b shows the point cloud of the pipe and the trajectory of the base frame of the drone during the experiment. The results obtained from the real-world experiments are similar to the ones obtained in the simulation environment.

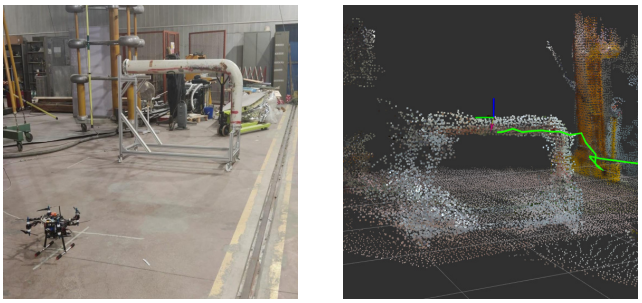

(a) (b)

Fig. 11: Environment in which the actual experiments were conducted. (a) The drone used and the pipe to be inspected are shown. (b) Dense reconstruction of the pipe from SLAM and drone base link

Figure 12 depicts the results obtained during a real-world experiment involving the tracking of a pipeline. The pink line represents the estimated central axis of the pipeline, which serves as a reference point for the drone's navigation. The green dot, meanwhile, represents the next tracking point that the drone uses to guide its movement along the pipeline. The black dot in the centre of the image represents the centre of the camera, and the goal is to align it with the axis so that its next position is the green dot. These images visually represent the drone's progress as it moves along the pipeline.

C. Defect detection

Figure 13 presents the results of corrosion detection on RGB images obtained during a real-case inspection process. The image shows several areas of corrosion, which are visible as discolouration or texture changes on the surface of the material. The blue lines in the figure delimit the areas of corrosion, making it easy to identify and quantify the extent of the damage.

It is worth noticing that the proposed approach to detect pipe defects represents a starting point with a relatively naive method. It is based on the assumption that the pipeline colour is consistent and distinct from the colour of the defects,

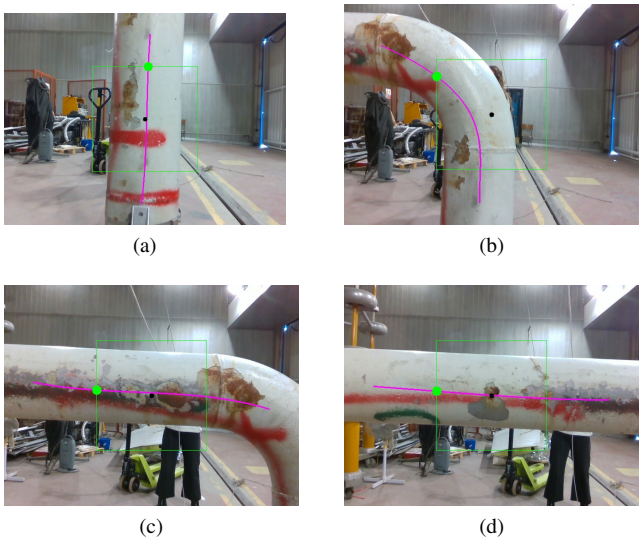

(a) (b) (c) (d)

Fig. 12: Results obtained in real experiments during the tracking of the pipeline. The pink line represents the central axis of the pipeline and the green dot is the next tracking point used to guide the drone.

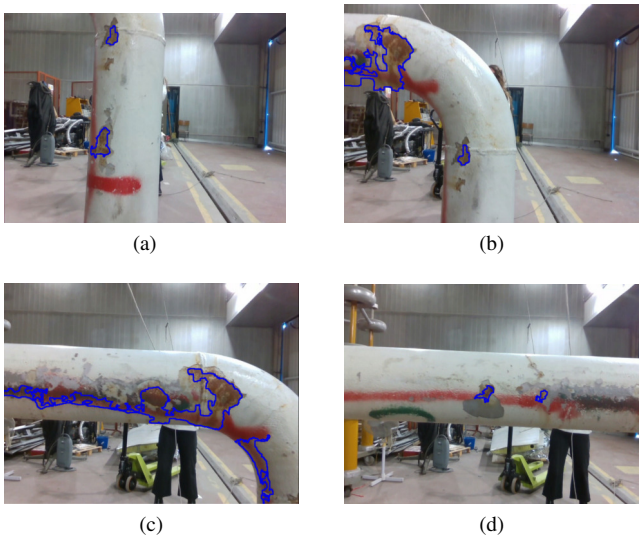

(a) (b) (c) (d)

Fig. 13: Corrosion detection results on RGB images obtained during the inspection process in real-case experiments. Defects are delimited by the blue lines

so it can fail to accurately identify the pipeline colour in certain situations, such as when the pipeline colour is not consistent or when some reflections or shadows affect the colour of the pipeline. In addition, it is only based on colour information. If the pipeline colour is not distinctive from the background, other information, such as shape or texture, should be considered. With machine learning techniques, it is possible to improve the accuracy and efficiency of the detection process. For example, deep learning algorithms such as convolutional neural networks (CNNs) can provide a more robust and automated approach to identifying image

defects.

Our approach can serve as a support tool for human workers by providing them with a quick and easy way to identify areas of corrosion on a surface. However, incorporating machine learning algorithms can increase the accuracy and efficiency of the detection process, making it more reliable and less dependent on human interpretation. With machine learning, the system can learn to detect subtle signs of corrosion that may not be visible to the human eye, and it can also handle a large amount of data for large-scale inspections. This can ultimately increase the effectiveness of the inspection process and reduce the risk of human error.

VI. Conclusion

This work presents a visual-based system to track and inspect industrial pipes using UAVs. The proposed approach utilizes a depth sensor to generate control data for the aerial platform to track the pipe following its central axis and detect possible defects. The system has been validated through a set of simulations and real experiments. The results of our experiments demonstrate that the proposed system can accurately track the central axis of the industrial pipe, allowing the detection of defects. In particular, our work focuses on external corrosion flaws. Further research is needed to enhance the system's accuracy and robustness, but this work provides a solid foundation for future advancements in this field. In addition, a more extensive evaluation with real-world experiments involving more complex pipeline structures, along with quantitative data, must be performed to better assess the inspection system's performance.

References

[1] H. H. Helgesen, F. S. Leira, T. A. Johansen, and T. I. Fossen, "Tracking of marine surface objects from unmanned aerial vehicles with a pan/tilt unit using a thermal camera and optical flow," in *2016 International Conference on Unmanned Aircraft Systems (ICUAS)*, pp. 107–117, 2016.

[2] M. Israel and A. Reinhard, "Detecting nests of lapwing birds with the aid of a small unmanned aerial vehicle with thermal camera," in *2017 International Conference on Unmanned Aircraft Systems (ICUAS)*, pp. 1199–1207, 2017.

[3] F. Furrer, M. Burri, M. Achtelik, and R. Siegwart, *RotorS—A Modular Gazebo MAV Simulator Framework*, pp. 595–625. Cham: Springer International Publishing, 2016.

[4] L. Joseph and J. Cacace, *Mastering ROS for Robotics Programming - Second Edition: Design, Build, and Simulate Complex Robots Using the Robot Operating System*. Packt Publishing, 2nd ed., 2018.

[5] P. Fazzini, J. Otegui, and H. Kunert, "Predicting failure conditions of smaw girth welded x70 pipelines subjected to soil movement," *International Gas Union World Gas Conference Papers*, vol. 4, 01 2009.

[6] G. RAMALLI, M. GIOVANI, F. PACCHIACUCCHI, and M. MANNESCHI, "Pipeline monitoring with drones.," *Studia Universitatis Babes-Bolyai, Ambientum*, vol. 61, 2016.

[7] L. Yu, E. Yang, P. Ren, C. Luo, G. Dobie, D. Gu, and X. Yan, "Inspection robots in oil and gas industry: a review of current solutions and future trends," in *2019 25th International Conference on Automation and Computing (ICAC)*, pp. 1–6, 2019.

[8] A. Kakogawa and S. Ma, "Design of a multilink-articulated wheeled inspection robot for winding pipelines: Airo-ii," in *2016 IEEE/RSJ International Conference on Intelligent Robots and Systems (IROS)*, pp. 2115–2121, Oct 2016.

[9] E. Dertien, S. Stramigioli, and K. Pulles, "Development of an inspection robot for small diameter gas distribution mains," pp. 5044 – 5049, 06 2011.

[10] E. Dertien, M. M. Foumashi, K. Pulles, and S. Stramigioli, "Design of a robot for in-pipe inspection using omnidirectional wheels and active stabilization," in *2014 IEEE International Conference on Robotics and Automation (ICRA)*, pp. 5121–5126, May 2014.

[11] "Inspection robotics." `[http://inspection-robotics.com/`. Accessed: 2021-06-26.

[12] B. Ross, J. Bares, and C. Fromme, "A semi-autonomous robot for stripping paint from large vessels," *I. J. Robotic Res.*, vol. 22, pp. 617–626, 07 2003.

[13] F. Yanqiong and S. Libo, "Design and analysis of modular mobile robot with magnetic wheels," vol. 3, pp. 902–911, 12 2008.

[14] J. C. Resino, A. Jardón, A. Gimenez, and C. Balaguer, "Analysis of the direct and inverse kinematics of roma ii robot," in *Climbing and Walking Robots* (M. O. Tokhi, G. S. Virk, and M. A. Hossain, eds.), (Berlin, Heidelberg), pp. 869–874, Springer Berlin Heidelberg, 2006.

[15] G. Wile and D. Aslam, "Design fabrication and testing of a miniature wall climbing robot using smart robotic feet," 01 2007.

[16] M. N. Mohammed, V. Shini Nadarajah, N. F. Mohd Lazim, N. Shazwany Zamani, O. I. Al-Sanjary, M. A. M. Ali, and S. Al-Youif, "Design and development of pipeline inspection robot for crack and corrosion detection," in *2018 IEEE Conference on Systems, Process and Control (ICSPC)*, pp. 29–32, 2018.

[17] J. Cacace, A. Finzi, V. Lippiello, G. Loianno, and D. Sanzone, "Aerial service vehicles for industrial inspection: Task decomposition and plan execution," *Applied Intelligence*, vol. 42, pp. 49–62, 01 2015.

[18] V. T. Hoang, M. D. Phung, T. H. Dinh, and Q. P. Ha, "System architecture for real-time surface inspection using multiple uavs," *IEEE Systems Journal*, vol. 14, no. 2, pp. 2925–2936, 2020.

[19] A. Lee, M. Dahan, and S. Amin, "Integration of suas-enabled sensing for leak identification with oil and gas pipeline maintenance crews," in *2017 International Conference on Unmanned Aircraft Systems (ICUAS)*, pp. 1143–1152, 2017.

[20] V. Lippiello and J. Cacace, "Robust visual localization of a uav over a pipe-rack based on the lie group se(3)," *IEEE Robotics and Automation Letters*, vol. 7, no. 1, pp. 295–302, 2022.

[21] H. Xiaoqian, H. Karki, A. Shukla, and Z. Xiaoxiong, "Variant pid controller design for autonomous visual tracking of oil and gas pipelines via an unmanned aerial vehicle," in *2017 17th International Conference on Control, Automation and Systems (ICCAS)*, pp. 368–372, 2017.

[22] P. Ravishankar, S. Hwang, J. Zhang, I. Khalilullah, and B. Eren-Tokgoz, "Darts—drone and artificial intelligence reconsolidated technological solution for increasing the oil and gas pipeline resilience," *International Journal of Disaster Risk Science*, vol. 13, pp. 1–12, 09 2022.

[23] B. T. Bastian, J. N, S. K. Ranjith, and C. Jiji, "Visual inspection and characterization of external corrosion in pipelines using deep neural network," *NDT & E International*, vol. 107, p. 102134, 2019.

[24] A. S. Saragih, F. Aditya, and W. Ahmed, "Defect identification and measurement using stereo vision camera for in-line inspection of pipeline," in *2022 Advances in Science and Engineering Technology International Conferences (ASET)*, pp. 1–5, 2022.

[25] C. Kratt, D. Woo, K. Johnson, M. Haagsma, P. Kumar, J. Selker, and S. Tyler, "Field trials to detect drainage pipe networks using thermal and rgb data from unmanned aircraft," *Agricultural Water Management*, vol. 229, p. 105895, 2020.

[26] R. Kafieh, T. Lotfi, and R. Amirfattahi, "Automatic detection of defects on polyethylene pipe welding using thermal infrared imaging," *Infrared Physics & Technology*, vol. 54, no. 4, pp. 317–325, 2011.

[27] J. Cacace, G. A. Fontanelli, and V. Lippiello, "A novel hybrid aerial-ground manipulator for pipeline inspection tasks," in *2021 Aerial Robotic Systems Physically Interacting with the Environment (AIRPHARO)*, pp. 1–6, 2021.

[28] A. Lopez-Lora, P. Sanchez-Cuevas, A. Suarez, A. Garofano-Soldado, A. Ollero, and G. Heredia, "Mhyro: Modular hybrid robot for contact inspection and maintenance in oil & gas plants," in *2020 IEEE/RSJ International Conference on Intelligent Robots and Systems (IROS)*, pp. 1268–1275, 2020.

[29] J. D. Foley, M. A. Fischler, and R. C. Bolles, "Graphics and image processing random sample consensus: A paradigm for model fitting with apphcatlons to image analysis and automated cartography," 1981.

[30] M. Labbé and F. Michaud, "Rtab-map as an open-source lidar and visual simultaneous localization and mapping library for large-scale and long-term online operation," *Journal of Field Robotics*, vol. 36, no. 2, pp. 416–446, 2019.